STRATIGRAPHY, SEDIMENTOLOGY, AND ISOTOPIC GEOCHEMISTRY OF AUSTRALIAN NEOPROTEROZOIC POSTGLACIAL CAP DOLOSTONES: DEGLACIATION, $\delta^{13}C$ EXCURSIONS, AND CARBONATE PRECIPITATION

MARTIN J. KENNEDY*
Department of Geology and Geophysics, University of Adelaide, S.A. 5005, Australia

ABSTRACT: **Thin (< 15 m) laterally persistent carbonate units cap glacial deposits in Neoproterozoic successions (1000–544 Ma) on almost every continent. Because these enigmatic carbonate units are typically isolated within siliciclastic successions, recurrently overlie successive glacigenic units, and define one of the most pronounced $\delta^{13}C$ excursions in the geologic record, they are interpreted to record a brief postglacial anomaly in ocean chemistry. In Australia, the Marinoan (Varanger equivalent ~ 600 Ma) cap dolostone units exhibit many of the characteristics displayed by such deposits elsewhere around the globe, including fine-grained dolomitic mineralogy, lateral persistence at basinal scales, thin laminae, graded beds, intervals with abundant marine cements, crystal fans, and a distinctive negative $\delta^{13}C$ isotopic signature of up to −5‰ PDB. On the basis of these features, the Australian examples are interpreted here to be deeper-water deposits (below storm wave base) resulting from an anomalous flux of inorganic carbonate to the sea floor during postglacial transgression. Detailed isotopic analysis of Australian cap dolostones indicates $\delta^{13}C$ values ranging from −1‰ to −5‰ and generally becoming more depleted in ^{13}C upsection. Trace-element data indicate some diagenetic stabilization, but textural evidence and the presence of similar profiles in different basins argue against a pervasive recrystallization event. The range in $\delta^{13}C$ values between sections as well as more negative $\delta^{13}C$ values appear to correlate with greater paleobathymetry within basins. This implies either (1) only partial preservation of the complete oceanic variation of $\delta^{13}C$ or (2) precipitation of this peculiar facies owes its genesis to basinal-specific oceanographic processes such as proximity of a given section to a postglacial upwelling zone. In the later case, $\delta^{13}C$ values would not represent whole ocean values.**

Stratigraphic constraints and paleoenvironmental interpretations suggest that much of this excursion lies within the geologically brief period of postglacial transgression. This implies that the cause(s) of $\delta^{13}C$ variation likely operated on time scales significantly less than the residence time of carbon in the oceans (10^5 yr). The continent-wide and perhaps global nature of cap dolostones indicates that large volumes of carbonate were precipitated during the postglacial transgressive period. Such large-scale carbonate precipitation over the hypothesized short time interval of postglacial transgression must have caused (or have been the product of) profound changes in the carbon cycle and global climate at that time. Similar evidence for transgression and increased carbonate deposition in the Holocene are attributed to the changing basin shape and pH of the oceans (the Coral Reef Hypothesis of Berger 1982). Cap dolostones may record a Proterozoic equivalent of this process with the substitution of abiotic carbonate precipitation for skeletal precipitation by reef organisms.

INTRODUCTION

The Neoproterozoic was an interval of dramatic change within the biosphere. This interval marked the transition from a series of extreme global ice ages that may have seen ice sheets at the Equator (Schmidt and Williams 1995) to climatic warming that was closely timed with the first appearance of the Ediacaran fauna (Cowie and Brasier 1989; Hofmann et al. 1990; Knoll and Walter 1992; Grotzinger et al. 1995). To understand the relationship between these events, researchers use Neoproterozoic carbonate successions as a record of paleoclimatic and oceanographic information (e.g., Knoll et al. 1986). Particular attention is paid to the $\delta^{13}C$ record, which provides both a potential mechanism for environmental interpretation and a monitor of paleoceanographic and atmospheric interaction, as well as an independent means of interbasinal correlation (Anderson and Arthur 1983; Knoll et al. 1986; Derry et al. 1992). The $\delta^{13}C$ marine record through this interval is as dramatic as the extraordinary evolutionary and atmospheric events at that time, and shows some of the largest shifts in Earth history. This record is dominated by extended periods of heavy values (+8‰) that periodically fall to very light values (down to −5‰) (Knoll et al. 1986; Kaufman and Knoll 1995).

The control on these excursions in the $\delta^{13}C$ record remains largely speculative, although the largest shifts are closely timed with glacial events. The most extreme of these shifts approximately coincides with the Varanger-age glaciation, and, within the limit of current data, appears to be defined exclusively by distinctive "cap dolostone units"; except for these cap dolostones, there are no reported negative values from rocks of approximately Varanger age within stratigraphically and diagenetically well controlled sections (Knoll et al. 1986; Fairchild and Spiro 1990; Kaufman et al. 1991; Smith et al. 1994; Narbonne et al. 1994; Kaufman and Knoll 1995). These thin, enigmatic dolostone horizons are almost ubiquitous capping Neoproterozoic glacial successions. Because of their $\delta^{13}C$ signature, distinct lithology, and potential as a climatological or biological marker, they are increasingly important in interbasinal correlation (Christie-Blick et al. 1995).

The presence of cap dolostones is well documented in Neoproterozoic successions throughout the world (Deynoux and Trompette 1976; Link 1983; Fairchild and Hambrey 1984; Eisbacher 1985; Tucker 1986; Preiss 1987; Aitken 1991; Siedlecka and Roberts 1992; Hegenberger 1993; Narbonne et al. 1994; Smith et al. 1994). They are typically thin (< 15 m) and laterally continuous at basinal scales. In siliciclastic-dominated sections they often constitute the sole carbonate interval, and in sections showing evidence for multiple glacial events, they typically overlie each glacial succession. A curious set of sedimentological features is associated with cap dolostone units independent of where the succession is located. This uniformity strongly suggests that cap dolostones share a similar depositional origin.

Published paleoenvironmental studies of cap carbonates are few. However, where studied, they have been ascribed to a variety of environments: lacustrine (Walter and Bauld 1983; von der Borch et al. 1989), supratidal (Plummer 1978; Williams 1979; Link 1983; Hegenberger 1993), subtidal storm-emplaced (Tucker 1986; Fairchild et al. 1989), and below storm wave base (Kennedy 1993). Similarly, description of the contact with the underlying glacial unit ranges from gradational (Plummer 1978; Williams 1979; Kennedy 1993) to erosional (von der Borch et al. 1989; Christie-Blick et al. 1990; Fairchild 1993; Dyson and von der Borch 1994). The various and often contradictory interpretations of the paleoenvironment influence arguments surrounding the origin of cap carbonates and affects their utility for interbasinal correlation. Outstanding questions remain as to the range and predominant depositional environment(s), temporal relationship

* Present address: Department of Earth and Space Sciences, University of California, Los Angeles (UCLA), Los Angeles, California 90024-1567 U.S.A.

JOURNAL OF SEDIMENTARY RESEARCH, VOL. 66, NO. 6, NOVEMBER, 1996, P. 1050–1064
 1073-130X/96/066-1050/$03.00

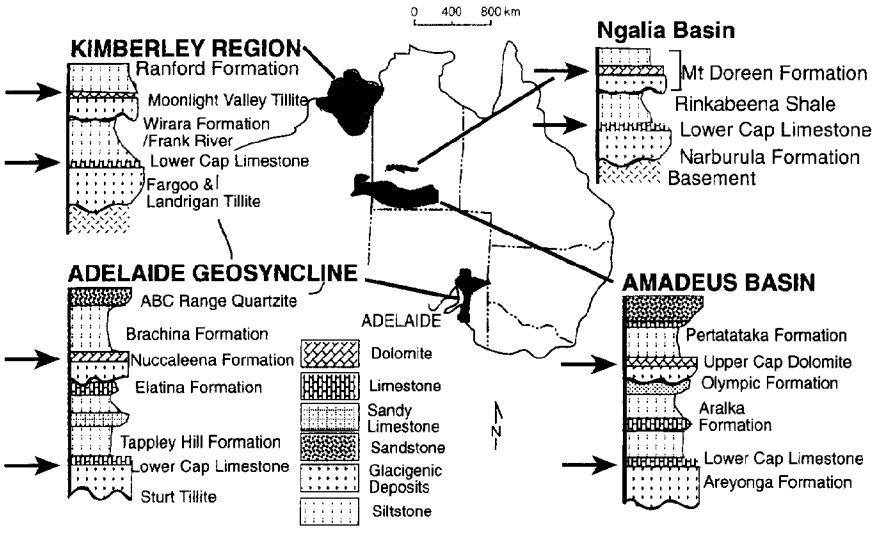

FIG. 1.—Basins containing Neoproterozoic postglacial carbonate units addressed in this paper. Black arrows indicate postglacial carbonate horizons.

to the underlying glacigenic succession, and origin of the pronounced $\delta^{13}C$ excursion recorded within these units.

Within the Neoproterozoic of Australia two major glacial units are preserved, both overlain by thin carbonate horizons (Preiss 1987). The purpose of the present study is to use Australia's uniquely well-preserved and laterally continuous record of cap dolostones to conduct both intrabasinal and interbasinal comparisons of facies and geochemical trends (Fig. 1). Worldwide, the Australian cap dolostones are arguably the most familiar examples of these peculiar horizons, and are a strong candidate for placement of the "Golden Spike" defining the base of the global stratotype section for the Vendian System (Knoll and Walter 1992). The ambition here is to reconsider the Marinoan age (Varanger equivalent) cap dolostone in order to reconcile conflicting paleoenvironmental information and to construct a general model for the origin of these units. Such a model would prove useful for both future interbasinal comparisons as well as investigations into the relationship between deglaciation, widespread carbonate deposition, and shifts in $\delta^{13}C$, characteristic of most Neoproterozoic sections.

STRATIGRAPHIC OCCURRENCE

Within Australia, distinct postglacial carbonate horizons are traceable from the Adelaide Geosyncline in the southern margin of the craton through the Amadeus and Ngalia Basins in the center of the continent to the Kimberley region in the north (Preiss et al. 1978). The great lithologic similarity of these cap carbonates has provided a basis for correlation between basins (Preiss et al. 1978). This study focuses mainly on the upper postglacial carbonate horizon in the Amadeus Basin, although comparative data are presented from the Adelaide Geosyncline, the Ngalia Basin and the Kimberley region.

Two Neoproterozoic glacial successions are present within the Amadeus Basin, both of which are overlain by thin carbonate horizons (Fig. 1; Preiss et al. 1978). The stratigraphically older (Sturtian) carbonate unit is a black, rhythmically laminated, organic-rich, peloidal limestone. The younger of the two cap carbonate units is better developed and crops out as a well-defined strike ridge at many localities within the basin. In the Neoproterozoic Umberatana Group of the Adelaide Geosyncline, two major glacial successions are also recognized, the older Sturtian glacials and the younger Marinoan glacials (Preiss 1987). Again, both glacial successions are capped by thin dolostone units, the younger Marinoan cap dolostone being the better developed. Two glacigenic intervals are also present in the Ngalia Basin and The Kimberley region, where thin dolomite horizons cap the upper interval of glacigenic deposits constituting the Mount Doreen Formation in the Ngalia Basin and the Moonlight Valley Tillite in the Kimberley region. On the basis of the lithostratigraphic similarity of these successions, Preiss et al. (1978) correlated the two glacial units of the Amadeus Basin with those of the Ngalia Basin, the Kimberley region, and the Adelaide Geosyncline. In the latter, both glacial successions lie below the well documented Ediacarian soft-bodied fossil assemblages.

The upper cap dolostone of the Amadeus Basin occupies the uppermost part of the glacigenic Olympic Formation. The Olympic Formation is composed predominantly of dolomitic siltstones, sandstones, and conglomerates of fluvial and mass-flow origin with rare striated clasts and lonestones (Field 1991). The cap dolostone of the Olympic Formation is conformably overlain by the laminated reddish-gray siltstones of the Pertatataka Formation. A very similar lithologic succession is present in the other basins in which the cap dolostone overlies glacigenic deposits and is conformable beneath laminated siltstones (Fig. 1; Preiss 1987).

PALEOENVIRONMENTS OF THE CAP DOLOSTONE

The Cap Dolostone of the Amadeus Basin

The upper cap dolostone of the Amadeus Basin is best represented in the northeastern corner of the basin, where it is 0–30 m thick (Fig. 2). The unit is a pure dolostone weathering to a light tan-brown. Its lower contact has erosional relief of up to several meters where it onlaps basement rocks along the northern margin and glacigenic conglomeratic facies (Olympic Formation) within the Basin. In the type section (Fig. 2), the contact with the Olympic Formation is poorly exposed but the base of the cap dolostone appears conformable and fines upward from shaly-parted dolomicrite to pure dolomicrite with minor Fe-rich stromatolites in the uppermost part of the unit. The contact with the overlying reddish-green siltstones of the Pertatataka Formation is sharp to transitional across a series of thin, intercalated, lime mudstone beds. There is no evidence of erosion along this upper contact.

The cap dolostone can be subdivided into four distinct lithofacies. Lithofacies I consists of cyclic centimeter-scale beds of dolomicrite with a variable component of reddish-gray terrigenous silt forming shale partings. Beds have sharp, commonly erosional bases, and are normal graded with either current-ripple cross-laminated or parallel-laminated tops (Fig. 3A, B). Unidirectional current marks are common at the bases. These marks are similar to flute casts in shape and scale but differ in that they formed as positive features on top of dolomicrite bedding planes. Previously described positive-relief flute marks are aligned parallel to paleocurrent di-

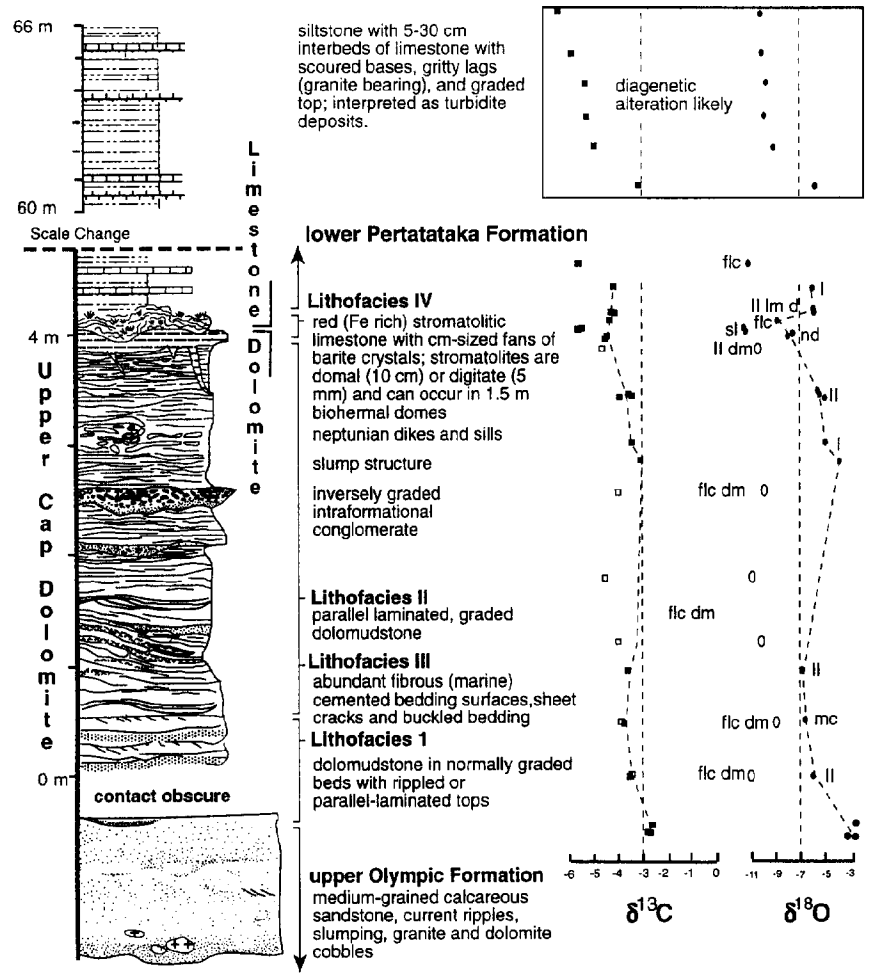

FIG. 2.—Measured section and isotopic profile of the cap dolostone overlying the glacigenic Olympic Formation in the northeastern Amadeus Basin; type section of the Olympic Formation. Key to abbreviations (also for Figs. 7–10): II = Lithofacies II; lm = light colored mud; dm = dark colored mud; ls = limestone; nd = neptunian dike; st = stromatolite; flc = allochthonous material; dr = muddy drape; int = internal sediment; mc = marine cement; w = visibly weathered; d = duplicated sample; C = conglomerate clast.

rection and flair downcurrent, similar to more standard negative-relief flute marks (Friedman and Sanders 1974). Repetitive successions with erosional bases, massive graded units, rippled intervals, and flat-laminated tops occur in an order corresponding to "A", "B", "C", and "D" units of the Bouma sequence. Terrigenous material is concentrated at the bases of these successions and grades upward into laminated dolomicrite with a crystal size of 5–50 μm with a mean of ~ 15 μm. Small (15 cm) anticlinal folds are present within flat-lying beds at one locality (Mt. Capitor, 25 km south of the type section) and resemble small tepee structures. The cores contain no space-filling cement. Their axes are parallel to those of larger, outcrop-scale folds, which are present only within carbonate units.

Lithofacies II is recognized by the uniform parallel-laminated, finely crystalline dolomicrite, which weathers to light tan. Laminae are 0.2–10 mm thick (Fig. 4A). Normal grading is common. Irregular dissolution surfaces with relief of up to 10 cm crosscut parallel-laminated dolomicrite. Topography along dissolution surfaces is filled and onlapped by subsequent laminae, suggesting synsedimentary formation. Poorly defined peloidal fabrics are common, suggesting that much of the dolomicrite was deposited as peloidal aggregates (Fig. 4B). Terrigenous silt is also present. The crystal size of the dolomicrite is 3–30 μm with a mean of ~ 10 μm. In the region near the type section of the Olympic Formation, Lithofacies II is extensively disrupted by semi-plastic asymmetric slumping and contains tabular, intraformational clasts, present in lenticular, inversely graded beds.

Lithofacies III is characterized by abundant fibrous cements that bound size-graded beds and form isopachous rims within cavities. Cement-lined cavities formed within the hinges of asymmetric slumps as well as between clasts. Fractures (neptunian dikes and sills) are commonly filled with dolomicritic internal sediments and fibrous (now dolomite) cements. Within cavities and fractures, successive horizons of cement are overlain by dolomicritic internal sediment, indicating a synsedimentary origin. Single-crystal palisade cements overlie size-graded beds and grade into more thickly cemented sheet cracks. More heavily cemented areas are associated with buckled and thrusted bedding (Fig. 5A, B, C).

Lithofacies IV is a distinctive stromatolitic boundstone composed of finely laminated lime mudstone. Stromatolitic fabrics include discrete columnar and laterally linked columnar forms with individual columns 2–20 mm in diameter. Fenestral fabric is not present. Large (10–200 cm) domal stromatolitic masses are also present. The stromatolitic masses are commonly silicified and/or ferruginized. Barite is commonly associated with the stromatolites, either as isolated bladed crystals (100–200 mm long) or as large upward-oriented rosettes of bladed crystals (up to 4 cm high) (Fig. 6). Crystals occur both in upright fans on the surface of microbial domes and without a preferred orientation within the peloidal micritic matrix of the dome itself. Individual barite crystals are white with numerous inclusions resulting in cloudy gray areas with undulose extinction. Crystal growth is repetitive, with an increasing percentage of crystals upward into a horizon of baritic fans. Fans are overlain by a successive micritic interval. Crystals grew at the sediment–water interface, as indicated by the upward-oriented growth habit, sediment drape defining crystal terminations, and presence of crystal fragments as detrital material within overlying sediment. Smaller-

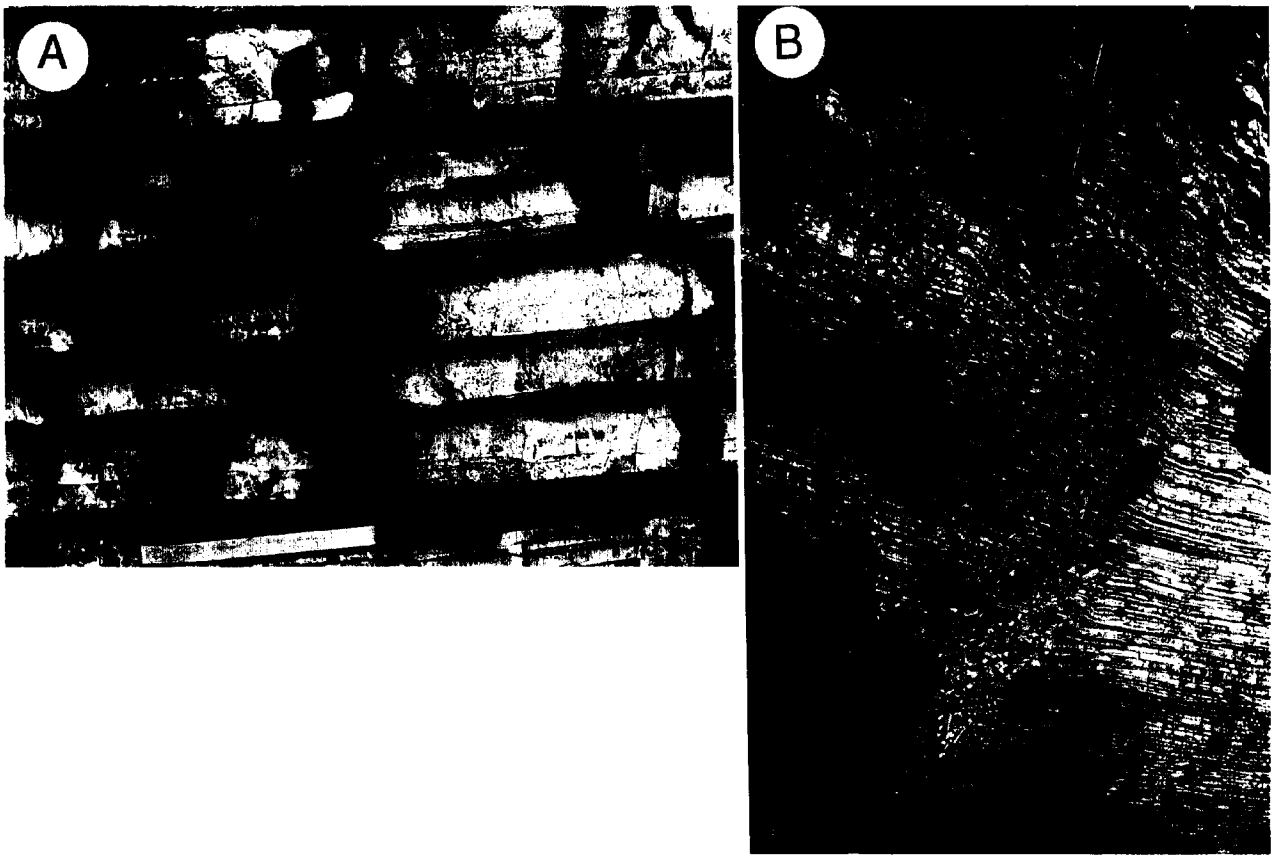

FIG. 3.—**A)** Graded bases, laminated tops, and darker-colored silty drapes, corresponding with Bouma A, B, C, and D divisions constituting a thick postglacial succession of **B)** rhythmically laminated beds (lithofacies I) at Mt. Capitor in the Amadeus Basin. This succession is interpreted as distal turbidite deposits.

scale randomly oriented crystals crosscut disrupted larger crystals occurring in fans, suggesting a later subsurface origin for these crystals.

Continuous strike ridges oriented at a sharp angle to the paleobasin margin enable cap dolostone units to be traced laterally within the Amadeus Basin. From the basin margin, sandstone and conglomerate are traceable down dip and change progressively to thinner-bedded fine sandstone, siltstone, and finally the interbedded siltstone and dolomicrite of Lithofacies I (Kennedy 1993). Farther in the basin, Lithofacies I thins and wedges out, thereby placing Lithofacies II sharply and erosionally on the top surface of the Olympic Formation glaciomarine deposits. In these more distal sections, Lithofacies III and IV are well developed. Where Lithofacies I is well developed, Lithofacies III and IV are absent. Where Lithofacies I is poorly developed, Lithofacies III and IV may be only partially represented. Lithofacies IV invariably occupies the uppermost parts of the cap dolostone beneath the red shales of the Pertatataka Formation whereas Lithofacies I typically occupies the basal unit. No lonestones were identified in the cap dolostone in the Amadeus Basin, although cobble-size conglomerate clasts form a lag deposit at the base of the unit.

Cap Dolostone Horizons in Other Regions of Australia

Field and petrographic examination of the Nuccaleena Formation of the Adelaide Geosyncline reveals remarkable lithologic similarities with the cap dolostones of the Amadeus Basin. The Nuccaleena Formation sharply overlies an irregular surface with up to 1 m of relief. The base in many places is a conglomeratic lag deposit. No lonestones were identified above the basal contact. Partial erosion of the underlying glacigenic succession may have preceded deposition of the Nuccaleena (Coats 1973; von der Borch et al. 1989). Lithologic equivalents of all the lithofacies described above are present although equivalents of III and IV are rare. Although barite fans have not been identified, relict crystal fans (now dolomite) show an acicular radiating form that may have been precipitated as aragonite. In one locality, the entire 2 m thickness of the cap is composed of Lithofacies IV limestone, which passes into Lithofacies II and III dolomicrite over 50 m. Synsedimentary fracturing, slump structures, tabular intraformational conglomerate, unidirectional positive-relief flute marks, and dissolution surfaces are abundant. Fibrous dolomite (marine) cements and internal sediment line synsedimentary fractures.

Tepee-like structures are common in the Nuccaleena Formation. They are cusp-shaped anticlinal forms with axes up to 1 m high connected by broad synclines up to 4 m wide. Linked structures form a parallel series of similar-scale folds continuous over kilometers. Subsequent laminae thin over the crests of these folds. No synsedimentary, space-filling cements are present in the cores of these structures. Positive-relief flute marks are subparallel to the tepee axes, but tepee axis orientation also correlates with regional tectonic trends. The bases of these large-scale tepee-like structures are defined by the subtle first appearance of shale partings at the bases of beds.

Lithofacies III is well developed at the base of the Nuccaleena Formation in many localities. Locally, laminated and graded beds of Lithofacies II dolomicrite are overlain by single-crystal layers of palisade fibrous cements. Laterally these beds may be split by sheet cracks with progressively increasing thickness of interlayer fibrous marine cements. Increasing abun-

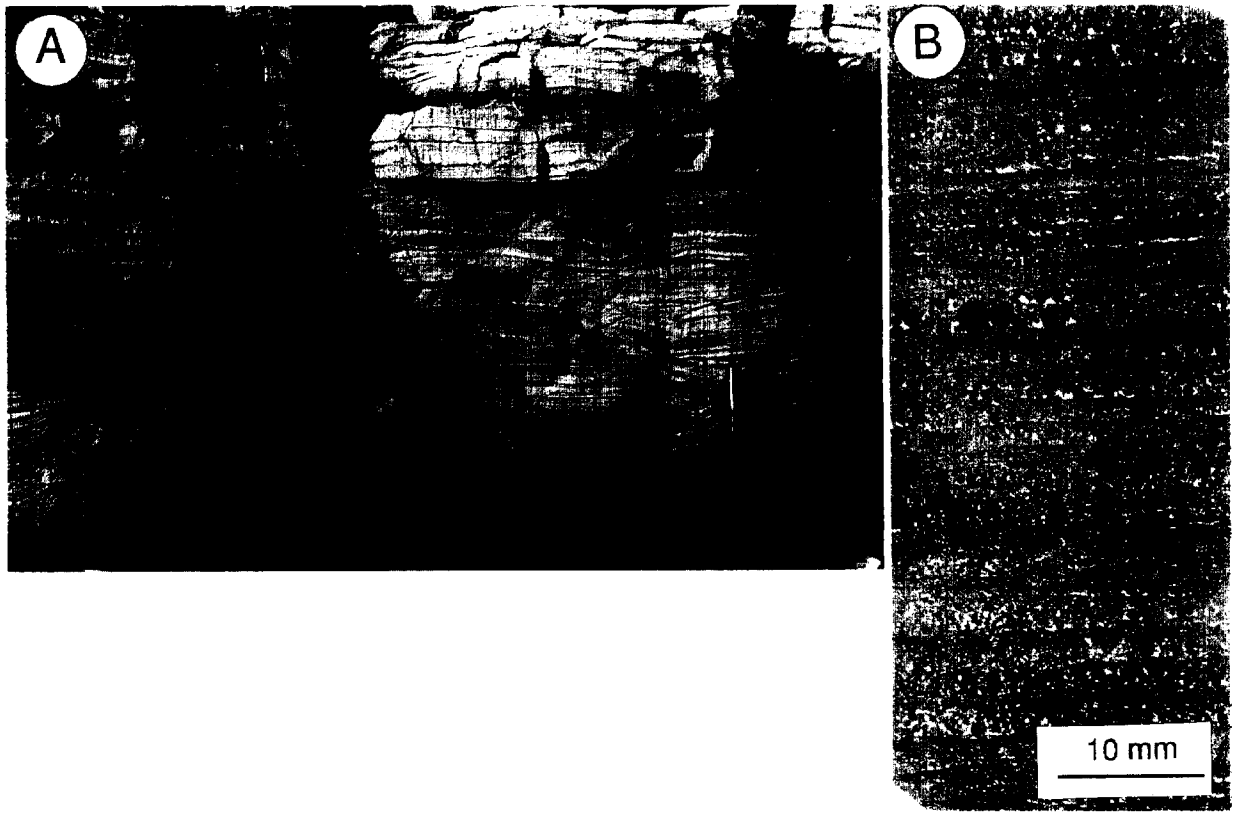

FIG. 4.—**A)** Typical appearance of Lithofacies II including thin lamination and graded beds, Mt. Doreen Formation, Ngalia Basin. **B)** Graded beds of peloidal dolomite constituting Lithofacies II, Olympic Formation type section, Amadeus Basin.

dance of cements is associated with further disrupted bedding and culminates in broad domal buckles. Domes are up to 0.8 m high, have cement and internal sediment-filled cavities within the hinges, are circular in plan view with no preferred orientation, and are onlapped by laminated dolomicrite. The best examples show rupture, thrusting, and fragmentation of the bedding. Tabular fragments are coated with multiple generations of fibrous marine cements, suggesting progressive synsedimentary disruption. Dissolution (hardground) surfaces are present in laterally equivalent, undisrupted Lithofacies II sediments and have up to 20 cm of relief. These irregular surfaces are onlapped by subsequent Lithofacies II laminae, indicating synsedimentary formation.

Within the Ngalia Basin, a cap dolostone unit sharply overlies diamictite of the glacigenic Mount Doreen Formation (Fig. 7; Preiss et al. 1978). Field data indicate that all four lithofacies found within the Amadeus Basin, including the baritic stromatolite facies (Lithofacies IV) and the sheet-cracked heavily marine-cemented lithofacies (Lithofacies III) are present. Neptunian dikes and sills are also abundant. Walter and Bauld (1983) noted the presence of barite and stromatolites within the Ngalia cap dolostones and suggested that the barite had replaced anhydrite, although they were unable to identify diagnostic crystal terminations. No lonestones were identified above the basal contact in this study.

The cap dolostone overlying the Moonlight Valley Tillite in the Kimberley region also shows a remarkable similarity of lithofacies to the examples from the Amadeus Basin described above, including cycles of terrigenous material and laminated dolomicrite with incomplete Bouma sequences (Lithofacies I), discrete intervals of sheet cracking (Lithofacies III), slumping, buckles, and tepee-like structures (Figs. 8, 9). The two sections presented from this region (Fig. 8, 9) show that a range of different lithofacies exists laterally within the same cap dolostone unit (as in the Amadeus Basin). The variation correlates with the paleobasin position of the two sections. Striated pavements underlying the Moonlight Valley Tillite indicate ice movement from northeast to southwest and imply that the paleo-basin deepened in that direction (Dow and Gemuts 1969). Southwestward deepening is also indicated by northeast–southwest-oriented current lineations and east-oriented flute marks in the cap dolostone and overlying Ranford Formation. Sections measured along the north–south-trending Osmond Range thus provide an oblique transect through the paleo-basin margin (Fig. 10). In the northern most proximal section near Turkey Creek (Fig. 9), the upper cap dolostone comprises sharp-based cycles of pure dolomicrite grading upward into fine-grained terrigenous material. Ripple cross-stratification is common in the middle and upper parts of these cycles; tepee-like structures and marine cements are absent. Shoaling cycles are thinnest at the base and thicken toward the top of the section before passing into the overlying clastic succession of the Ranford Formation.

Southward (basinward) at Palm Springs, carbonate intervals are more prominent and show a more typical assemblage of sedimentary structures and lithofacies, including partial Bouma sequences, laminated dolomicrite with prominent sheet cracks, marine cement, and tepee-like structures (Lithofacies III). Tepee-like structures are particularly well developed. Tepee-like structures are up to 1 m in height with fibrous cement lining conglomerate clasts within the cores. Lonestones were not identified at Palm Springs or the Turkey Creek type section, but are reported elsewhere in the Kimberley region (Williams 1979).

INTERPRETATION OF SEDIMENTARY ENVIRONMENT

Most researchers favor a shallow-water environment of deposition (lagoonal, lacustrine, or peritidal) for the Australian postglacial cap dolo-

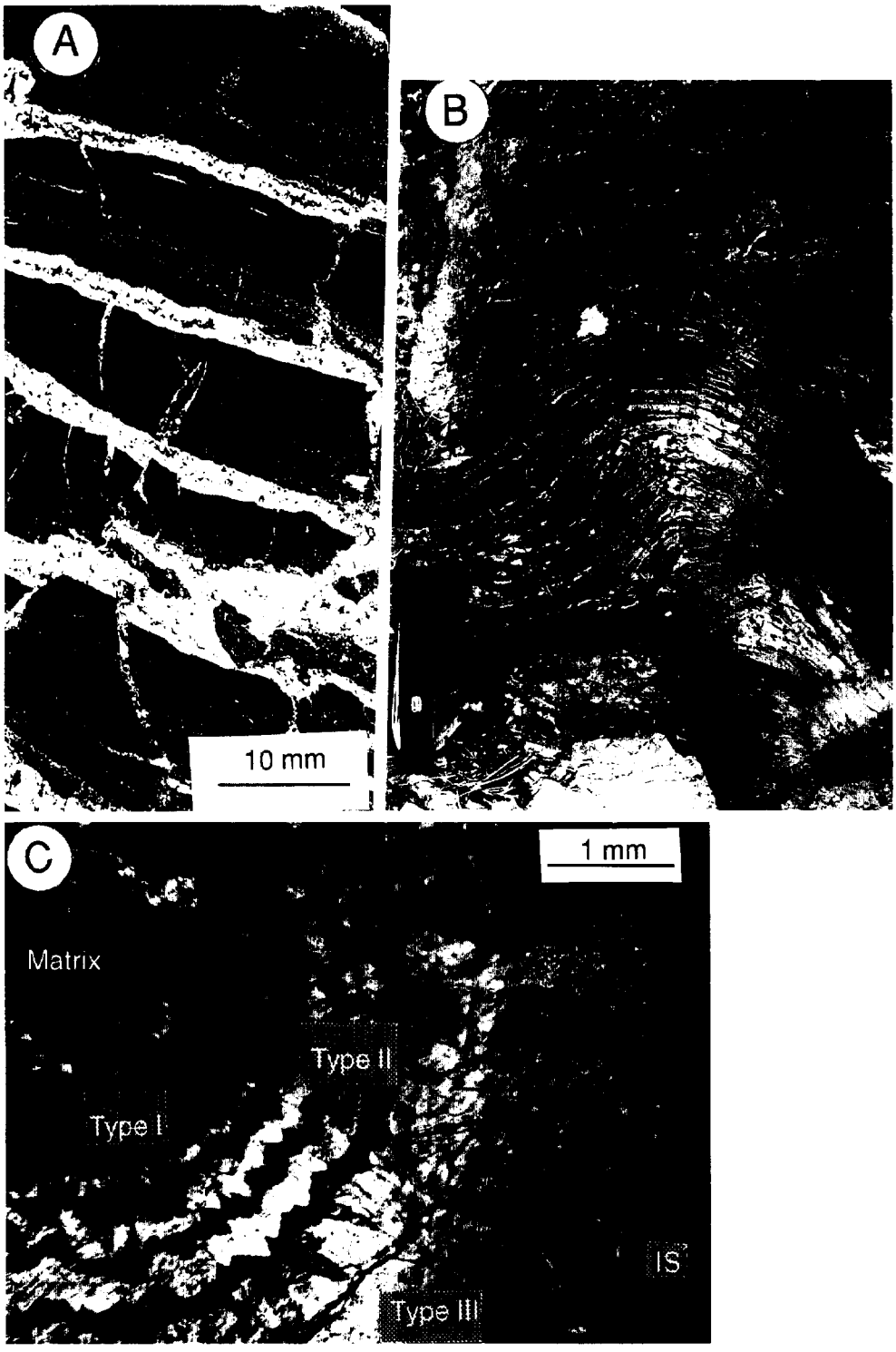

FIG. 5.—**A)** Graded beds overlain by cement suggesting carbonate cementation between depositional events; Cleary Creek, Amadeus Basin. **B)** A domal form composed of bedding planes lined by marine cement; such domes lie on a continuum between palisade cement-lined beds and buckled and thrusted beds with cement filled cores at this locality; Mt. Chambers Gorge, Flinders Ranges. **C)** Photomicrograph of fibrous marine cements and internal sediments from the Olympic Formation type section, Amadeus Basin. Crossed nicols, showing micritic type I, growth banded type II, and columnar type III cements, which are overlain by internal sediments (IS).

FIG. 6.—Upward-growing baritic fans overlain by micrite. Thick section is 9 cm wide. Cleary Creek, Amadeus Basin.

stones. For the Nuccaleena Formation in the Adelaide Geosyncline, Plummer (1978) suggested a predominantly peritidal environment of deposition largely from the presence of erosional tops to beds, tepee structures, and stromatolites. On the basis of algal and cryptalgal lamination, tepee structures, and intraclastic beds, Williams (1979) suggested a predominantly supratidal to lagoonal origin for cap dolostones from the Kimberley region and the Adelaide Geosyncline. von der Borch et al. (1989) suggested the cap dolostones of the Adelaide Geosyncline to be transgressive lacustrine deposits similar to modern alkaline ephemeral lakes and sabkha deposits of the Coorong region. Walter and Bauld (1983) suggested a lacustrine environment of deposition for cap dolostones of the Amadeus and Ngalia Basins, on the basis of similarities with modern sediments in Antarctic lakes.

A number of features of the cap dolostones, however, are not consistent with a shallow-water origin, including the presence of graded beds with well-defined Bouma sequences, abundant slump features, thin laminae, and sole marks. The lateral persistence of cap dolostone units at basinal to interbasinal scale does not support a lacustrine environment. Sedimentary structures typical of shallow depositional settings are absent from the cap dolostones, including tidal features, desiccation structures, and fenestral fabrics. It is suggested here that the cap dolostones were deposited under widespread basinal conditions predominantly below storm wave base in a relatively shallow intracratonic sea. A deeper-water origin for the cap dolostones is consistent with deglaciation and the overall transgressive nature of the succession overlying the Marinoan glacial succession.

The normally graded, shale-parted dolomicrites of Lithofacies I are interpreted as event beds of possible storm or turbidity-current origin. The parallel-laminated dolomicrites of Lithofacies II are suggestive of pelagic to hemipelagic or periplatform oozes deposited in a basinal setting. The common co-association of slump features, mass-flow textures, and reworked conglomerate clasts suggests gravitational slope instability of partially lithified sediment. Fracturing during interlayer gravity sliding within these semiconsolidated units may have resulted in formation of neptunian dikes and sills.

Tepee-like structures in the cap dolostones of the Adelaide Geosyncline have been taken as strong evidence for a shallow-water origin (Plummer 1978; Williams 1979). Although the scale and general form of these structures is similar to the classic shallow-water tepees of Kendall and Warren (1987), they show important differences. The tepees within the cap dolostone have longitudinal rather than polygonal plan shape and may not be synsedimentary. While some examples appear to be onlapped by subse-

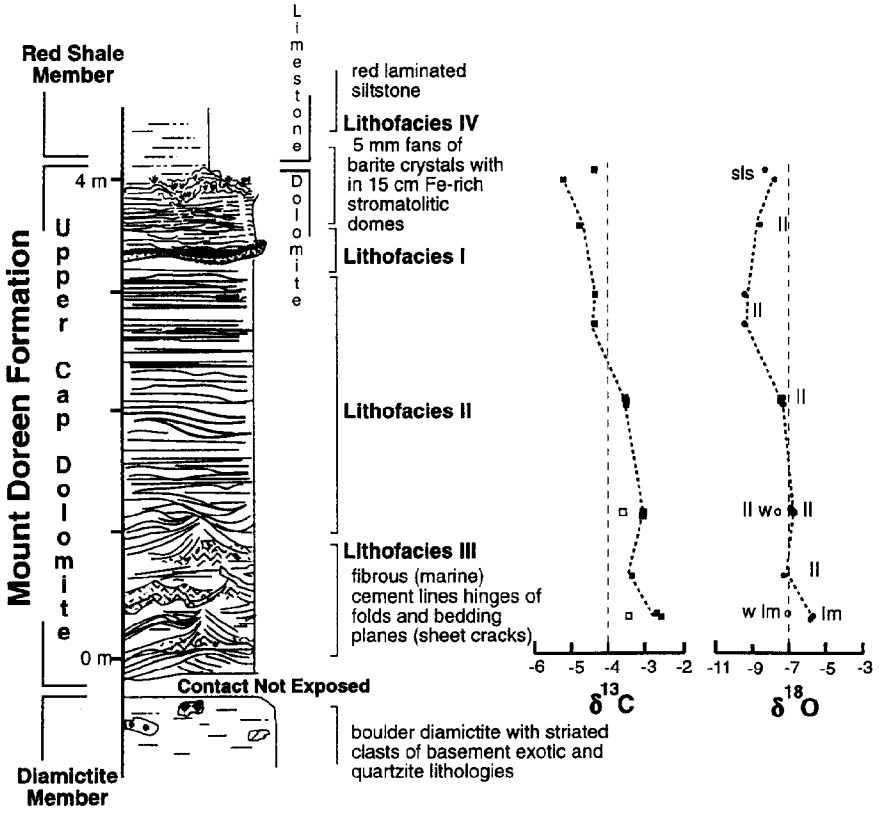

FIG. 7.—Measured section and isotopic profile of the upper postglacial carbonate horizon overlying glacigenic rocks in the Mt. Doreen Formation at its type section in the Ngalia Basin. See Figure 2 for key to abbreviations.

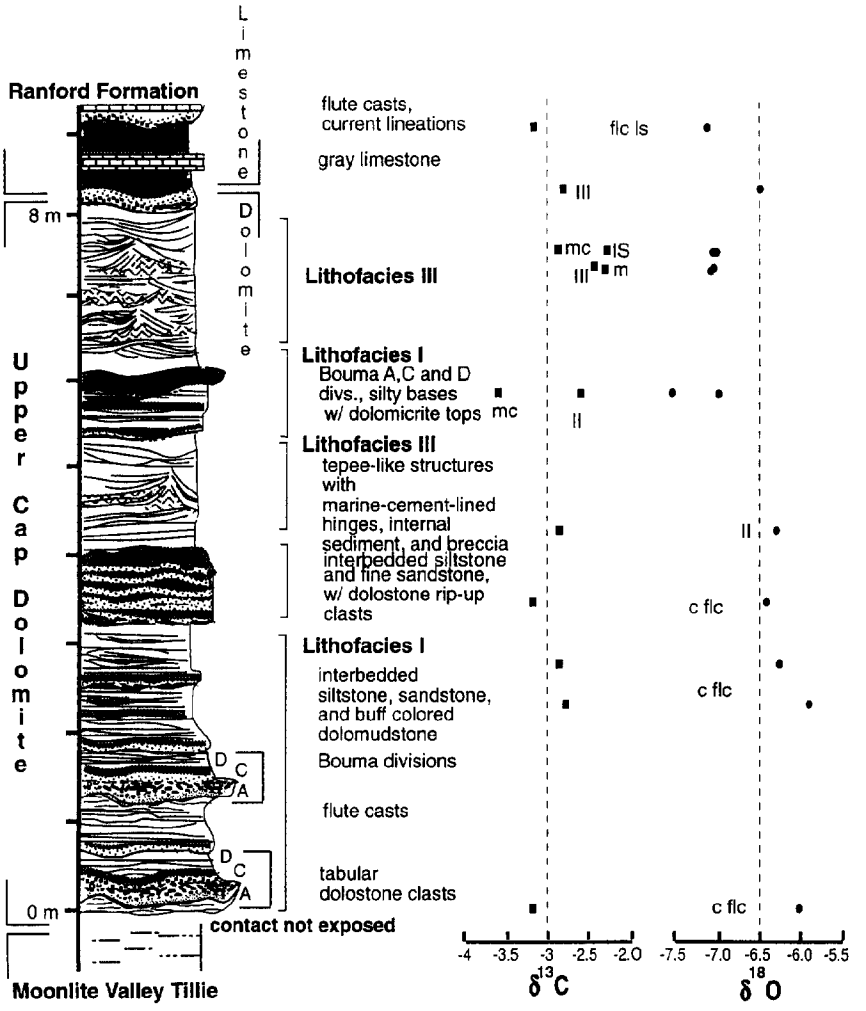

FIG. 8.—Postglacial carbonate horizon overlying the Moonlight Valley Tillite south of Halls Creek at Palm Springs in the Kimberley region (19° 43′ S lat., 127° 48′ E long.). See Figure 2 for key to abbreviations.

quent units, all examples (within the Adelaide Geosyncline) lack synsedimentary space-filling cements in their cores. In continuous outcrop exposure, they form kilometer-scale sheets of continuous parallel folds that are subparallel to regional tectonic trends (which in the Amadeus Basin can be directly related to outcrop-scale tectonic folds). An alternative origin for these tepee-like structures is disharmonic folding between the overlying and underlying more competent clastic units. A third possible origin is suggested by the correlation of the axes of these structures with the positive flute marks, implying some relationship to paleoslope. Exactly what this relationship might be is unclear, however, because the current marks indicate that the fold axes were parallel to paleoslope, 90° to the expected orientation of gravity-induced slide- or slump-related folding. Although these structures are enigmatic, they are not unique. Almost identical tepee-like forms are described within a similar thin cap dolostone unit (the tepee dolostone) that overlies Varanger-age glacial deposits in the Mackensie Mountains of Canada (Aitken 1991).

Distinctive domal structures and buckled bedding in Lithofacies III are associated with an increase in fibrous marine cement between bedding planes. Laterally over 10–100 m, undisturbed laminated and graded beds of Lithofacies II pass from bedding planes lined with single-crystal palisade cement to interbedded intervals of fibrous cement up to 1 cm thick. The cement lines cavities within the crests and hinges of domes as well as coating clasts within centimeter-scale disrupted and thrusted bedding. Such domes have previously been interpreted as stromatolites (Plummer 1978). Beds within these domes, however, are typical of Lithofacies II laminated and graded intervals and do not show evidence of crenulated lamination or increased number or thickness of laminae toward their crests, as would be expected in stromatolitic buildups. Instead, the increase in space is created by the greater abundance of early diagenetic fibrous cement along with internal sediment-filled cavities between beds. The discrete stratigraphic intervals in which these heavily cemented horizons are present suggest low sedimentation rates. Condensation is also suggested by the dissolution surfaces in these same intervals. Coeval dissolution and cementation suggests that dissolution occurred on the sea floor, while cement precipitation probably occurred from carbonate-supersaturated solutions beneath the sediment/water interface.

The stromatolites within the cap dolostone in the Amadeus and Ngalia Basin have many similarities with deep-water forms present as crusts and hardgrounds in deeper-water environments (Playford et al. 1976; Dromart 1992). These include a finely laminated, nonfenestral microstructure, lack of microbial flake breccias, and abundance of iron oxide. The stromatolitic carbonates of Lithofacies IV are interpreted as deep-water, possibly bacterial stromatolites, which grew in a sediment-starved environment and represent a highly condensed interval. The barite within the stromatolites may be analogous to that in the ferruginous stromatolites of a condensed Lower Cambrian carbonate succession in South Australia (Wallace et al. 1991).

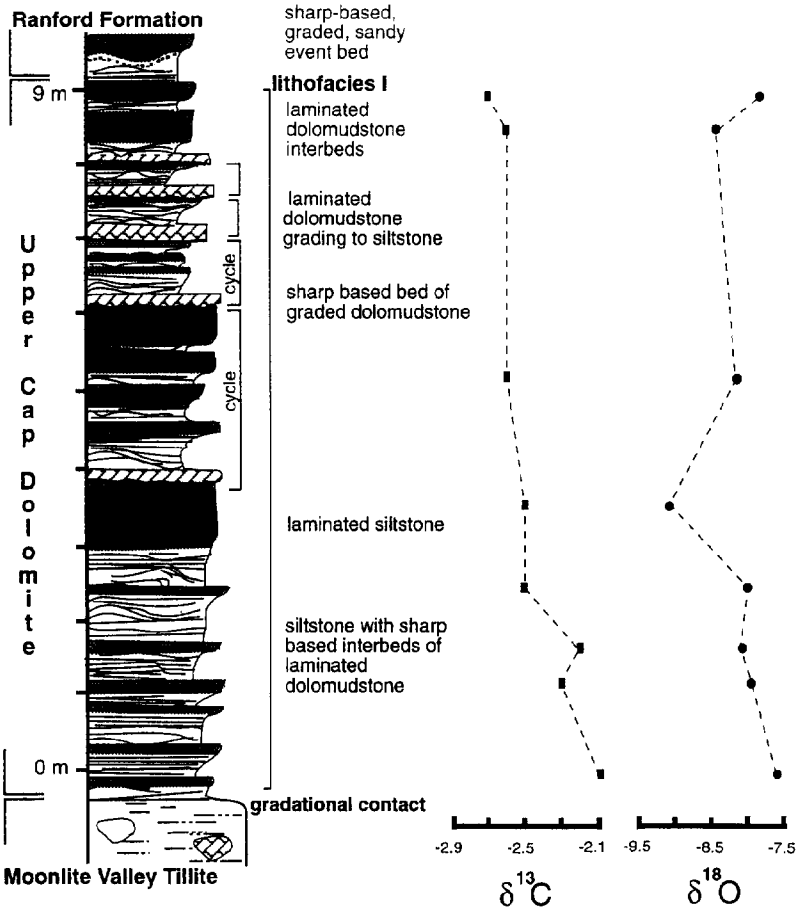

FIG. 9.—Measured section of the postglacial horizon overlying the Moonlight Valley Tillite in the type section east of Turkey Creek, Kimberley region. See Figure 2 for key to abbreviations.

Barite is suggested here to be a primary chemical sediment on the basis of sedimentary and crystallographic relationships. Barite deposition in deeper-water (below storm wave base) settings is known from the modern marine record (Paytan and Kastner 1994; Deharis et al. 1980) and is thought to be concentrated during periods of high oceanic productivity (Dymond et al. 1992). Precipitation of barite crystals requires both $(SO_4)^{2-}$ and free Ba^{+2} ions; these ions are more readily available in an oxidizing environment and indicate the presence of free oxygen during precipitation of these crystals.

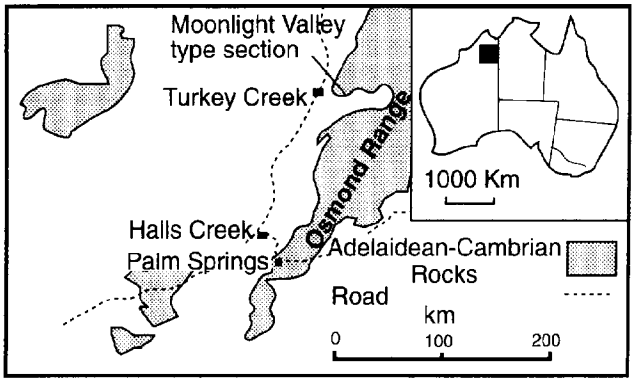

FIG. 10.—Locality map of the Kimberley region showing relative position of measured sections east of Turkey Creek and near Palm Springs in the Osmond Range (after Preiss and Forbes 1981).

Cap dolostone units are interpreted to be transgressive deposits on the basis of the abrupt shift to fine-grained facies, change to a deeper-water environment of deposition, onlap of the paleobasin margin, and stratigraphic position between coarse-grained shallow marine and terrestrial deposits of the glacigenic succession and conformably overlying marine siltstone deposits. Cap dolostone units are suggested to be the product of background carbonate precipitation (condensation) in areas with limited terrigenous input. Lithofacies I represents the transition of initial terrigenous input to pelagic/hemipelagic precipitation of Lithofacies II with continued flooding, shutdown of carbonate precipitation, and sediment starvation resulting in deposition of Lithofacies IV. In sequence-stratigraphic terms, the cap dolostones represent a condensed transgressive system tract. The deep-water stromatolites overlying the cap dolostones constitute a highly condensed maximum flooding surface lying below the prograding mudstones of the overlying highstand sediments. The condensed interval is not developed in more proximal localities, where the top of the transgressive deposits are composed of thin shoaling-upward cycles that thicken upward into highstand sediments.

This interpretation requires the proximal time-equivalent facies of the cap carbonate to be marine siliciclastic rocks. This relationship is supported by lateral facies changes observed in the Amadeus Basin (above) as well as cap dolostone units overlying the Moonlight Valley Tillite in the Kimberley region. In the Kimberley Region the variation of cap dolostone units between the measured sections reflects a transition from storm-wave influence in the proximal section to deposition below storm wave base in the more distal southern section. Near Turkey Creek, shoaling-upward cycles are interpreted as parasequences developed along the basin margin. Sharp-

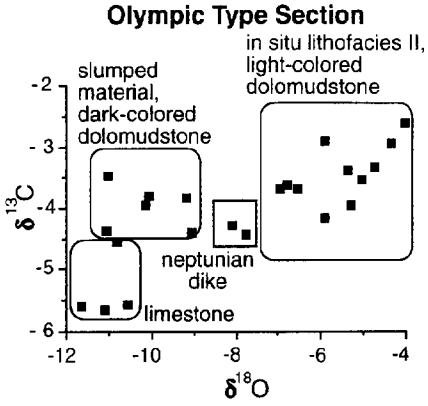

FIG. 11.—Stable-isotope values of different facies within the Olympic Type Section (Amadeus Basin) showing depletion of $\delta^{18}O$ in slumped material (darker colored, ferric) and stromatolitic limestone.

based dolomitic intervals comprise flooding surfaces deposited as background sedimentation during periods of limited input of terrigenous material coupled with a period of anomalously high carbonate precipitation within the water column (Van Wagoner et al. 1990). Analogous dolomite-capped parasequences are described within the Sea Cliff Sandstone of the Adelaide Geosyncline, a possible basin-margin equivalent of the cap dolostone overlying the Marinoan glacigenic succession in this region (Nuccaleena Formation) (Dyson and von der Borch 1994).

Southward in the deeper parts of the Kimberley basin, minor cycles merge resulting in fewer shoaling-upward cycles. The presence of unreworked turbidite deposits within the terrigenous component suggests deposition below the influence of storm reworking. The presence of fibrous marine cements, tabular intraclasts, and semiplastic slumps indicates partial lithification within the carbonate intervals.

In the Amadeus Basin, the base of the cap dolostone oversteps the paleobasin margin and fills meter-scale erosional relief where it overlies glacigenic and basement rocks. Laterally time-equivalent clastic rocks along the basin margin lie within incised valleys, indicating that a period of erosion preceded deposition of the cap dolostone (Kennedy 1993). The Nuccaleena Formation in the Adelaide Geosyncline has similarly an erosional lower contact; there, both meter-scale relief and regional truncation of the underlying glacigenic rocks have been documented (Coates 1973; von der Borch et al. 1989; Christie-Blick et al. 1990; Fairchild 1993; Dyson and von der Borch 1994) and interpreted as a correlative sequence boundary to that underlying the cap dolostone in the Amadeus Basin (Christie-Blick et al. 1995).

The pervasive erosion surface that separates the cap dolostone from the underlying glacigenic deposits challenges the genetic relationship of these units. Should this surface represent an extended hiatus, then the presence of carbonate rocks immediately overlying glacial deposits is simply coincidental. Direct evidence of glacial influence or ice retreat such as dropstones is largely absent in cap carbonate units. Although lonestones have been documented in the Adelaide Geosyncline and the Kimberley region (Plummer 1978; Williams 1979) none were observed above the basal contact in this study and some previously reported lonestones were present only along the basal contact of the unit. These are reinterpreted as a transgressive lag conglomerate. Unequivocal examples of dropstones may yet exist in the more isolated regions of the Kimberley region (G. Williams, written communication 1992), but the general absence of lonestones suggests that ice rafting was not important during deposition of the lower part of the cap dolostone.

A purely coincidental relationship between carbonate deposition and deglaciation seems unlikely, however, given (1) the stratigraphic position of

TABLE 1.—*Geochemical data from cap dolostones in the Amadeus and Ngalia Basins and the Kimberley Region. Refer to Figure 2 for the key to symbols.*

Number	Lithology	Height (m)	$\delta^{13}C$ (‰)	$\delta^{18}O$ (‰)	$^{87}Sr/^{86}Sr$	Sr (ppm)	Mn (ppm)	Fe (ppm)	Mg/Ca	carb (%)
Amadeus Basin: Olympic Formation Type Section										
Base of Cap Dolostone										
3-7-91-1	II dr		−7.2	−2.9	−5.9	0.71506	108			75
3-7-91-1	d		−7.2	−2.9	−5.9					75
3-7-91-2	II flc		−5.7	−2.6	−4.0					88
3-7-91-3A	dm flc		0.0	−3.5	−11.0		65	1528	6680	0.64	79
3-7-91-3b	lm flc		0.0	−3.6	−6.8	0.71148	73				78
3-7-91-4	flc		0.4	−3.9	−9.2						84
3-7-91-4a	f c		0.4	−3.7	−6.5						
3-7-91-5	II dr		0.9	−3.7	−6.9						55
3-7-91-6	II dr		1.3	−3.8	−10.0	0.71588	123				78
3-7-91-7	dm		1.8	−4.4	−11.0		79	6320	19380	0.44	83
3-7-91-9	dm flc		2.6	−4.0	−10.1						75
3-7-91-10	t		3.0	−3.6	−5.0		85	1593	2147	0.48	60
3-7-91-11	II lm dr		3.6	−4.0	−5.2						65
3-7-91-12	flc		4.2	−4.4	−9.0	0.71452	92	1696	5240	0.43	75
3-7-91-13	II lm dr		4.4	−3.0	−4.3		227	1703	2113	0.42	69
3-7-91-13	d		4.4	−3.4	−4.7						67
3-7-91-14	II lm dr w		3.6	−3.4	−5.3		117	1905	4080	0.42	76
3-7-91-14	d II dr		3.6	−3.6	−5.5						
3-7-91-15	nd		4.0	−4.6	−10.8		73	2395	5520	0.45	87
3-7-91-16a			4.2	−4.3	−8.1	0.71321	186	3440	12480	0.45	69
3-7-91-16b	nd (matrix)		4.2	−4.4	−7.7		132	11080	14380	0.41	79
3-7-91-17a	st ls		4.2	−5.6	−11.6	0.70929	398	2200	1471	0.01	41
3-7-91-17b	st ls		4.2	5.5	−11.6		120	2273	1722	0.09	76
Top of Cap Dolostone											
3-7-91-18	flc		1.6	−4.2	−5.9		91	2402	5160	0.40	62
3-7-91-20	ls		6.4	−5.7	−11.1	0.71327	97	1702	817	0.01	70
3-7-91-22	ls		60.0	−3.1	−5.5						60
3-7-91-23	ls		60.8	−5.0	−9.2						57
3-7-91-24	ls		62.4	−5.3	−10.2						
3-7-91-25	ls		63.2	−5.3	−10.1						75
3-7-91-27	ls		64.0	−5.4	−10.2	0.71641					58
3-7-91-28	ls		64.8	−6.3	−10.1						
25-6-91-12a	int. sed			−2.8	−8.2						51
25-6-91-12b	mc type I			−3.8	−8.9						65
25-6-91-12c	mc type II			−4.0	−10.5						75
25-6-91-12c	mc type II			−4.0	−10.5						
25-6-91-12d	mc type III			−3.2	−8.1						71
25-6-91-12e	dolospar			−3.1	−8.1						91
25-6-91-12f	matrix			−2.9	−8.2						61
Amadeus Basin; Wallara Core											
W/1	I	1272.0		−3.7	−8.2		61	2344	6100		42
W/2	I	1273.5		−4.4	−8.0						56
W/4	I	1275.0		−3.7	−8.4						66
W/5	I	1276.0		−3.5	−8.2		72	2071	9500		43
W/6	I	1277.5		−3.3	−8.0						64
Kimberley region; Palm Springs											
PS-A	flc	0.0		−3.2	−6.1		46	876	2623	0.53	84
PS-B	flc	2.6		−2.8	−6.0						73
PS-C	flc	2.8		−2.9	−6.2		44	816	2223	0.50	80
PS-D	II	3.4		−3.2	−6.4		61	871	2227	0.53	76
PS-E	II	4.3		−2.7	−6.3		62	686	1562	0.52	66
PS-F	II	5.8		−2.6	−7.0		63	374	1430	0.53	66
PS-I	III	7.4		−2.4	−7.2		46	1067	3980	0.53	77
PS-J	III	8.2		−2.8	−6.5		41	526	2586	0.50	86
PS-k	flc;ls	10.0		−3.1	−7.1						70
PSF	Mc type II	5.8		−3.1	−7.5						95
PS-20a	mc type II	7.4		−2.7	−8.8						81
PS-20b	mc type I	7.4		−2.9	−8.6						93
PS-20c	matrix	7.4		−2.4	−7.1						77
PS-8a	mc type I	7.5		−2.8	−7.0						79
PS-8b	mc type II	7.5		−2.9	−8.6						87
PS-8c	int. sed	7.5		−2.4	−7.1						59
Kimberley region; Turkey Creek											
MLV-1	I	0.0		−2.1	−7.6		32	4000	3833	0.52	68
MLV-3	I	1.2		−2.3	−7.9						67
MLV-4	I	1.6		−2.2	−8.1		46	1639	2375	0.53	75
MLV-5	I	2.5		−2.5	−7.9		38	1258	1371	0.56	75
MLV-6	I	3.5		−2.5	−9.2						73
MLV-7	I	5.2		−2.6	−8.2		56	1470	2377	0.51	62
MLV-8	I	8.5		−2.6	−8.4						74
MLV-9	I	8.9		−2.7	−7.7		39	3060	1460	0.51	57

TABLE 1.—*Continued*

Number	Lithology	Height (m)	$\delta^{13}C$ (‰)	$\delta^{18}O$ (‰)	$^{87}Sr/^{86}Sr$	Sr (ppm)	Mn (ppm)	Fe (ppm)	Mg/Ca	carb (%)
Ngalia Basin										
22-8-91-1	lm	0.0	−2.9	−6.3	0.72511	60	2434	3663	0.51	71
22-8-91-1	d	0.0	−2.8	−6.2						74
22-8-91-1a	wlm	0.0	−3.4	−7.1						67
22-8-91-2	II	0.5	−3.6	−7.4						70
22-8-91-3A	IIw	1.2	−3.7	−7.8		70	2453	6120	0.49	63
22-8-91-3B	II	1.2	−3.3	−7.0		62	2147	5000	0.49	71
22-8-91-3B	d	1.2	−3.3	−6.9						
22-8-91-4	II	2.1	−3.6	−7.3	0.72535	67				69
22-8-91-4	d	2.1	−3.6	−7.3						70
22-8-91-4b	II	2.1	−3.6	−7.5						72
22-8-91-5	II	2.7	−4.4	−9.5						74
22-8-91-6	II	3.0	−4.4	−9.4		86	1868	5060	0.47	83
22-8-91-7	II	3.6	−4.9	−8.5		32	7360	4080	0.46	75
22-8-91-8	s ls	4.0	−5.3	−7.5	0.72541	163				67
22-8-91-9	s ls	4.2	−4.3	−8.4	0.72912	187	1420	1263	0.45	32

these carbonate units, which directly overlie glacial rocks and typically are the only carbonate unit in these otherwise siliciclastic successions, (2) their presence overlying almost every example of Varanger-age glacial deposits described around the world, and (3) their transgressive origin within a part of the succession in which a glacioeustatic rise would be expected. The alternative interpretation is that their basal surfaces do not represent extended periods of time, but instead formed in response to deglacial processes such as glacio-isostatic rebound (Kennedy 1993) and/or high-order eustatic oscillations similar to those documented during Pleistocene deglaciation (Fairbanks 1989). Further documentation of the scale and characteristics of these erosion surfaces is necessary to better resolve the genetic relationship of these units with glaciation.

In Australia, the younger Neoproterozoic cap dolostones appear to be nearly identical in the Adelaide Geosyncline, the Amadeus and the Ngalia Basins, and the Kimberley region. Many postglacial carbonate horizons documented from other parts of the world share remarkable similarities with the distinctive sedimentary structures in the Australian example: These include microcrystalline grain size, peloidal aggregates, tepee-like structures, discrete intervals of sheet cracking and marine cement-lined laminae, common repetitive graded beds, millimeter-scale laminae, and presence of crystal fans. Deeper-water interpretations include those of Tucker (1986), who reported sub-wave-base features in the postglacial limestones overlying the Kingston Peak Formation in California; Fairchild and Hambrey (1984), who interpreted a transgressive origin for Varanger-age postglacial dolostones in Spitsbergen; Christie-Blick et al. (1989), who questioned the shallow-water features previously reported in postglacial carbonates in the Pocatello Formation of Southern Idaho; and Dyson and von der Borch (1994), who suggested the Sea Cliff Sandstone of the Adelaide Geosyncline to be time equivalent to the Marinoan cap carbonate unit (Nuccaleena Formation) and of a deeper-water origin. Excepting some equivocal examples of fine-grained dolostones overlying glacial deposits in California and central Namibia (Cloud et al. 1974; Hegenberger 1987), it is more likely that cap dolostones are of a deeper-water origin, deposited as background sedimentation during transgression. Time-equivalent, shallow-water facies are then suggested to be composed of terrigenous sediment. The virtually global similarity of cap dolostone units likewise implies a more laterally continuous, deeper-water origin rather than a localized, peritidal or lacustrine facies as proposed in previous studies.

GEOCHEMISTRY AND DIAGENESIS OF THE CAP DOLOSTONE

In the stratigraphic profiles presented below, $\delta^{13}C$ results are internally consistent and broadly correspond to values thought to reflect primary marine variation reported from other continents (Kaufman and Knoll 1995). High-resolution analysis from within the cap carbonate interval shows a range in $\delta^{13}C$ values between sections as well as a consistent trend of ^{13}C depletion upsection within individual stratigraphic profiles. If these trends record variation of marine water (a "Varangian Event") they provide a means of independently assessing lithostratigraphic correlation between geographically isolated postglacial successions as well as reflecting oceanic processes during deglaciation.

Methods

Both textural components and bulk samples corresponding to stratigraphic position were collected in the Amadeus and Ngalia Basins and the Kimberley region. Samples were studied using cathodoluminescence and plain-light microscopy and analyzed for C, O, and Sr isotopic values and Fe, Sr, Rb, Mn, and Ca content. Samples were collected in type sections as well as additional localities with particularly good exposure. Some samples were analyzed from the Wallara 1 core in the southwestern Amadeus Basin in order to compare the effects of surficial weathering. Samples were collected every 30–100 cm within stratigraphic profiles. Bulk samples were slabbed and powder was extracted away from obviously weathered zones with a dental drill, reacted with 100% H_3PO_4 at 50°C (dolomite) and 25°C (limestone) for 12 hr, and analyzed on a Micromass 602 E stable isotope mass spectrometer with an internal accuracy of 0.1‰. Some samples were duplicated, and powder was taken from differing areas of the sample to verify reproducibility and homogeneity within a given hand sample. Textural components were drilled from thin-section rough cuts using a 500 μm drill bit viewed beneath a binocular microscope and analyzed using the method above.

Trace-element geochemistry was measured using 300 mg of powder derived from the above method, reacted with acetic acid, filtered using 54 hardened filter paper to remove any terrigenous component, and then analyzed using a Varian AA6 atomic absorption spectrophotometer. The limited available quantity of some textural components (principally marine cements) prohibited trace element analysis from being conducted.

Measurement of $^{87}Sr/^{86}Sr$ was conducted on some bulk rock samples from the Amadeus and Ngalia Basin. Samples were extracted using a dentist drill and 100 mg was dissolved in 1M HCl. The dissolved fraction was redissolved in 3M HCl and passed through cation exchange columns to extract Sr. Isotopes were analyzed on a Finnigan Mat 261 mass spectrometer. Rb content was measured using XRF on extra sample powder and found to be indistinguishable from minimum detectable concentrations of 15 ppm.

Petrography

Dolomicrite lithofacies of the cap dolostone (except Lithofacies IV) have a uniform, finely crystalline (3–30 μm) dolomicritic texture with a uniform light orange to red luminescence and up to 20% scattered terrigenous material composed of quartz and feldspar grains. Patches of microspar luminesce blue. Later-stage crosscutting fractures associated with manganese dendrites and ferroan staining luminescence bright yellow or blue and are bordered by euhedral-zoned dolomite crystals. Subsurface samples taken from the Wallara core were unweathered and devoid of these local fracture-related textures.

Cavity-lining dolomite fibrous cements are interlaminated with dolomicritic and terrigenous internal sediments. These cements are morphologically similar to isopachous fibrous cements commonly interpreted as being of early diagenetic marine origin in Phanerozoic limestones. Dolomite cements are present in all study areas and show good textural preservation, although they weather quickly and may be ferroan. Four varieties of cavity-lining cements are recognized: (I) dolomicritic, (II) growth-banded columnar radial fibrous, (III) radial fibrous, and (IV) equant blocky. Remaining cavity space is filled by either internal sediment or drusy dolospar (Fig. 5C; Kennedy 1993).

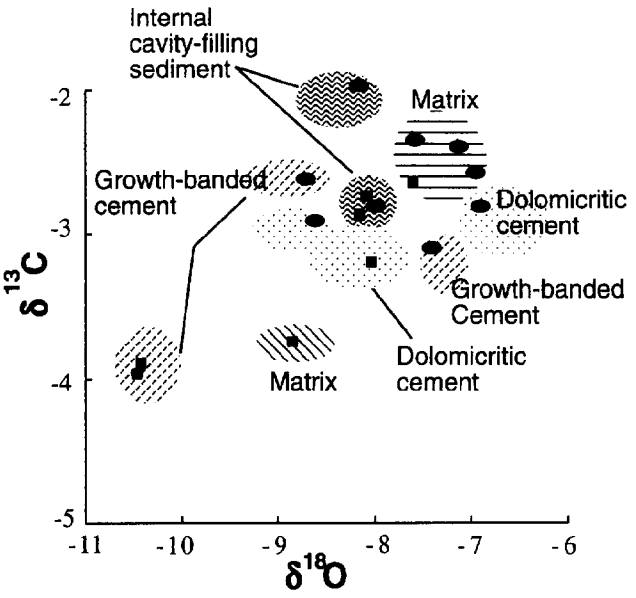

FIG. 12.—Stable isotopic values of different types of dolomite marine cement, matrix, and internal sediment from the Kimberley region and Amadeus Basin. Marine cements show a consistently lighter $\delta^{13}C$ and $\delta^{18}O$ than matrix material. Squares represent samples taken from the Amadeus Basin (Olympic Formation type section), and circles represent samples taken from the Palm Springs section in the Kimberley region.

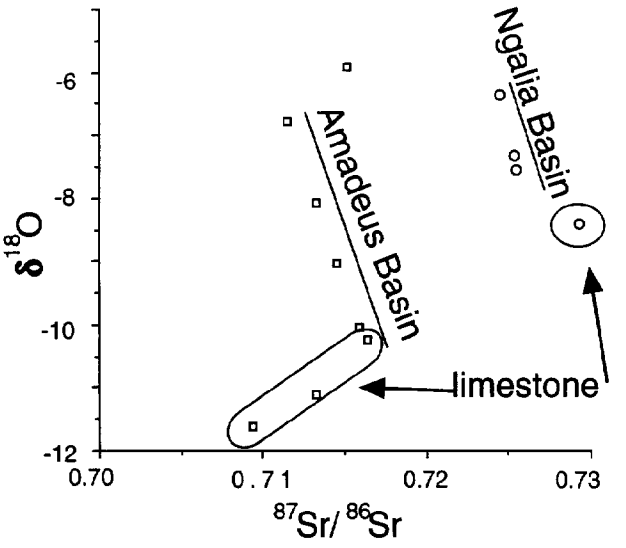

FIG. 13.—Cross plot of $^{87}Sr/^{86}Sr$ and $\delta^{18}O$ showing covariation between these isotopic systems in the Amadeus and Ngalia basins. Squares represent samples from the Amadeus Basin while circles represent samples from the Ngalia Basin.

Geochemical Results

$\delta^{13}C$ values of samples from all regions show depletion of ^{13}C from $-2‰$ to $-6‰$ PDB with respect to typical marine carbonates. $\delta^{13}C$ values within single profiles are largely consistent, and show similar trends in the various study localities. The magnitude of values, however, differs between sample localities. The important trends are as follows:

(1) ^{13}C is depleted upsection in most stratigraphic profiles (Figs. 2, 7, 9). ^{18}O within these same profiles show a divergent trend of enrichment upsection.

(2) Depletion of ^{13}C of up to $-1‰$ is associated with zoned euhedral dolomite crystals lining weathered fractures and darker-colored (ferroan) slumped units. These areas correspond to enrichment of Fe and $-5‰$ shifts in $\delta^{18}O$ creating covariant trends within parts of profiles that are weathered or slumped (Figs. 2, 11, Table 1).

(3) Negative shifts of $-1‰$ to $-1.5‰$ in $\delta^{13}C$ occur across the transition from dolomicrite to stromatolitic limestone at the top of the section, which is also associated with a $-6‰$ shift in $\delta^{18}O$ in stromatolitic material (Fig. 2). Lime mudstone interbedded with siltstones overlying the cap dolostone in the Pertatataka Formation at the Olympic Formation type section are highly weathered, show euhedral dolomite crystals, and contain a covariant trend between $\delta^{13}C$ and $\delta^{18}O$ with more negative values upsection (Fig. 2, Table 1; Sample #3/7/91/19-3/7/91/28).

(4) There is depletion of up to $-1‰$ ^{13}C within fibrous marine cements relative to surrounding dolomicrite and internal sediments (Fig. 12). Further depleted values by $-1‰$ ^{13}C and $-2‰$ ^{18}O correspond with inclusion-rich palisade-columnar cements in some samples. Bright-yellow luminescent veins extending from fractures follow the upper and lower contacts of palisade-columnar cements in this sample, indicating later fluid flow in these fractures. Similar fractures are associated with local neomorphic textures.

(5) $^{87}Sr/^{86}Sr$ is considerably more radiogenic relative to Proterozoic sea water values from other regions (Asmeron et al. 1991). ^{87}Sr covaries with $\delta^{18}O$ and total Sr ppm (Fig. 13, Table 1).

(6) There is no correlation between carbonate content and isotopic values for any group of samples measured.

Trace-element analysis from all localities indicates uniformly low Sr levels and abundance of Fe and Mn relative to modern sea water (Table 1). In both the Ngalia and Amadeus Basin, limestones and stromatolitic limestones have a greater concentration of Sr and smaller concentration of Fe and Mn than the underlying dolomites (Table 1).

Diagenetic Interpretation

Diagenesis appears to have affected standard geochemical markers of these rocks without homogenizing $\delta^{13}C$ values within individual sections or between depositional components, creating diagenetic fabrics, or affecting delicate textures of marine cements. Additionally, the persistence of $\delta^{13}C$ trends in separate basins across the craton more closely approaches the scale of oceanic processes than that of known diagenetic environments. Trace-element content of Fe, Mn, and Sr as well as dull luminescence, however, indicates a degree of diagenetic stabilization. The uniformly low Sr concentration (< 200 ppm) within the cap dolostone also points to diagenetic alteration (Veizer 1983). $^{87}Sr/^{86}Sr$ values are considerably more radiogenic than known Vendian sea-water values (Derry et al. 1989; Kaufman et al. 1993). Furthermore, $^{87}Sr/^{86}Sr$ covaries with both Sr concentration and ^{18}O depletion (Fig. 13). The dissimilarity of $\delta^{18}O$ and Sr concentration from marine water suggests alteration during diagenetic stabilization. This seemingly contradictory result is reported from other successions in which regionally extensive dolomitization reset both Sr and O isotopic systematics but did not significantly affect $\delta^{13}C$ values (Banner and Hansen, 1990; Banner et al. 1988; Magaritz 1985). Because carbon is a major component of carbonate rocks and a minor component of sedimentary fluids, the $\delta^{13}C$ signature of carbonates is much less susceptible to water-rock alteration than $^{87}Sr/^{86}Sr$ or $\delta^{18}O$. Consequently, carbonate successions that undergo diagenetic stabilization with a low water/rock ratio are unlikely to have $\delta^{13}C$ completely reset or homogenized.

Similar textural preservation coupled with nonmarine geochemical values for trace elements have been reported in the Neoproterozoic Beck Spring Dolomite and interpreted as very early diagenetic stabilization of a primary metastable high-magnesium calcite (HMC) or calcian dolomite (Tucker 1983; Zempolich et al. 1988). Delicate textures in the now dolo-

mite marine cements are most likely to be maintained by early alteration of a primary mineralogy high in Mg that stabilized directly to stoichiometric dolomite without an intervening calcite phase. Mimetic replacement of fine-grained material and marine cement further suggests that stabilization occurred with a low water/rock ratio. Abundant Fe, Mn, radiogenic Sr, and negative $\delta^{18}O$ values indicate that recrystallization occurred in the presence of reduced fluids more typical of local argillaceous material in a mixing or burial environment than marine water at the sea floor.

Whether stabilization to stoichiometric dolomite occurred from a primary HMC phase or a poorly ordered dolomite phase is unclear. Widespread precipitation of dolomite better explains the (now) ubiquitous dolomitic mineralogy, absence of diagenetic fronts within cap dolostones, and retention of delicate crystal textures. Evidence for Proterozoic primary dolomite remains equivocal, however, because kinematic arguments favor an origin of HMC or aragonite. Later mimetic replacement of HMC is facilitated by the fine grain size of the primary precipitate and a tendency of dolomite to faithfully maintain HMC textures. HMC has also been reported from possible correlative intervals in the Amadeus Basin (Walter and Bauld 1983).

TRANSGRESSION, CARBONATE PRECIPITATION, AND CO_2 RETURN

Evidence for widespread carbonate precipitation during postglacial transgression indicated by cap dolostone units suggests a similar oceanographic response described by the Coral Reef Hypothesis for deglaciation in the Holocene (Berger 1982; Opdyke and Walker 1992): a fall in sea level at the beginning of glaciation redirects bicarbonate flux from deposition as carbonate on the shelf to the deeper carbonate-undersaturated ocean, where it remains in solution. For each mole of bicarbonate not precipitated as $CaCO_3$ on the shelf (i.e., which remains in solution in deep water), the atmosphere is denied the return of one mole of CO_2. In this way, changes in ocean bathymetry can influence p_{CO_2} and enhance icehouse conditions. This imbalance is ultimately restored during postglacial transgression when bicarbonate-charged deep water floods the shelves and initiates rapid precipitation of $CaCO_3$ in the form of coral reef growth. In the case of Precambrian postglacial carbonate intervals, abiotic precipitation of carbonate is substituted for biogenic skeletal precipitation. In either case, once upwelling is initiated, $CaCO_3$ precipitation and associated CO_2 release acts as a positive feedback, accelerating warming and deglaciation. How upwelling and carbonate precipitation are initiated is less clear. However, given the increased saturation state of the Proterozoic ocean, the propensity for carbonate precipitation in the form of chemical whitings (Kempe and Degens 1985; Knoll and Swett 1990; Grotzinger and Kasting 1993) and the relative sizes of the oceanic and atmospheric reservoirs, it is not unreasonable that a whiting at a sufficiently large scale could have significantly altered p_{CO_2}, triggering deglaciation (Kennedy 1993). Unfortunately the resolution of the stratigraphic record is inadequate to determine whether inorganic carbonate deposits straddle the glacial-to-deglacial transition. Should a chemical whiting have initiated a return to interglacial p_{CO_2} levels, the resulting thin carbonate interval would be difficult to recognize. Further arguments to establish such an event will need to rest on quantitative models of bicarbonate flux.

CAP DOLOSTONES AND THE $\delta^{13}C$ EXCURSION

$\delta^{13}C$ values measured in cap dolostones discussed above are typical of the negative values for postglacial carbonates that overlie Varanger-age glacial deposits (Kaufman and Knoll 1995). Two classes of oceanic models have been proposed to account for this excursion. In the first, burial rates of ^{12}C-rich organic material decline in response to a slowdown in organic productivity in an increasingly stagnant postglacial ocean (Broecker 1982). Values recorded in marine precipitates reflect steady-state long-term variations in carbon composition of the upper ocean. In the second, opening of postglacial oceans invigorates oceanic circulation patterns (Kaufman et al. 1991). This acts to return ^{12}C to the water column by oxidizing organic sediments accumulated on the sea floor in a formerly anoxic deep ocean. Upwelling of deep water enriched in ^{12}C changes local or whole-ocean values (depending on mixing) for a brief interval determined by the residence time of carbon in the oceans, or about 10^5 yr (Kump 1991). This second class of models requires any excursion to be short lived, representing a simple reorganization of carbon already present in the oceanic reservoir.

Among the individual $\delta^{13}C$ profiles presented here, there is considerable range of isotopic variation recorded: from 4‰ in the Amadeus Basin to less than 1‰ in the carbonate horizon overlying the Moonlight Valley Tillite at Turkey Creek (Fig. 2, 9). Assuming $\delta^{13}C$ of cap dolostones are representative of whole ocean values, the variations of the isotopic curve from profile to profile may indicate an incomplete sedimentary record at any given sample locality. Such abbreviations of the broader $\delta^{13}C$ curve hypothesized for this time period (Kaufman et al. 1995) might result from the hiatus in deposition indicated by the erosional contact common at the base of the cap dolostone, or the position of a given isotopic profile with respect to the basin margin. Profiles from near paleobasin margins, such as Turkey Creek (Fig. 9), record only a part of the curve between initial transgression and downlap of the ensuing highstand deposits. More complete records showing a greater range of $\delta^{13}C$ are preserved in more distal localities such as at Palm Springs (Fig. 8). In accordance with this hypothesis, the stromatolitic interval, which is interpreted as a condensed section in the Ngalia and Amadeus Basins and the Adelaide Geosyncline, implies a considerable period of time between transgression and subsequent highstand. These units also correspond to the most negative $\delta^{13}C$ values.

If the cap dolostones provide a record of secular $\delta^{13}C$ variation, the negative values present in all sections likely reflect the late stage of transgression in the shallow, intracratonic, ramp-style basins characteristic of this study. It is then likely that a complete $\delta^{13}C$ record is preserved only in the deeper basinal positions that maintained continuous carbonate sedimentation throughout the period of decline to negative values.

Alternatively, the $\delta^{13}C$ trends can be explained with respect to basin position relative to postglacial upwelling zones of bicarbonate-saturated and ^{13}C-depleted deep water. Presumably, inorganic precipitation of carbonate from bicarbonate-saturated deep water would not take place in the upper ocean, but would occur progressively upward as deep water became metastable while rising into lower pressure and warmer upper ocean. Carbonate with the most negative $\delta^{13}C$ values would likely be precipitated in basinal areas nearest to the source of upwelling deep water. In localities farther from upwelling zones (i.e., more proximal basin settings), continued mixing of ^{13}C-depleted deep water with normal marine water would create the spatial and temporally variable signal present in the $\delta^{13}C$ profiles (such as those from the Kimberley region). For this mechanism, $\delta^{13}C$ values and carbonate precipitation are linked to the more local process of upwelling and do not reflect secular variation, but transgression.

The stratigraphic constraints of the cap dolostone (see earlier section) place the unit above the glacial deposits and beneath a maximum flooding surface. This implies that the part of the $\delta^{13}C$ excursion lying within this horizon is restricted to the time of transgression between ice-sheet ablation and sea-level highstand. Rate resolution in Proterozoic rocks is generally problematic, but by analogy with timing of deglaciation in the Holocene, glacioeustatic transgression likely occurred on time scales significantly less than 10^5 yr. Thus, for the portion of the curve associated with the cap dolostone, $\delta^{13}C$ appears to have changed fairly rapidly. For the entire $\delta^{13}C$ curve, which varies from +8‰ to −5‰ and back to +7‰ (Narbonne et al. 1994; Kaufman and Knoll 1995), the currently available stratigraphic and isotopic data are inadequate to place the curve within a stratigraphic framework. Further high-resolution stratigraphic and geochemical work is needed to locate the inflection points of the $\delta^{13}C$ curve relative to the

glacial event and to further test whether the negative $\delta^{13}C$ values are solely contained within cap carbonate horizons.

CONCLUSIONS

Sedimentological observations from the younger Neoproterozoic (Marinoan) cap dolostone unit of several Australian Basins (the Amadeus and Ngalia Basins, the Adelaide Geosyncline, and the Kimberley region) indicate a predominantly deeper-water (dominantly below storm wave base) environment of deposition. Cap dolostone units often gradationally overlie glacigenic deposits, suggesting a temporal relationship with glaciation within the basin. Laterally, toward the paleobasin margin, these units overlie erosional surfaces and interfinger with siliciclastic sediments before wedging out entirely. Within the deeper basin, the upper contact of the cap dolostone consists of deep water stromatolites and barite crystal fans which represent a thin, highly condensed interval corresponding with reduced carbonate deposition (sediment starvation) during maximum flooding. Overall, the cap dolostone records the interplay between accelerated background precipitation of carbonate material and terrigenous input along a shoreline during deglaciation and transgression.

The currently available isotopic data from this and other studies indicate that cap dolostones define the pronounced negative excursions in Neoproterozoic successions. Stratigraphic data presented here suggest that the carbonate was deposited during transgression, indicating that the process responsible for the extreme negative excursion may have been limited to the immediately postglacial period. If deglaciation in the Neoproterozoic was analogous to Holocene deglaciation, the duration of transgression is likely to have been shorter than the residence time of carbon in the oceans, thus supporting non-steady-state oceanographic models for the origin of these deposits. Further detailed stratigraphic and isotopic studies in other basins around the world are needed, however, to better establish the inflection points of the isotopic curve relative to the glacial period and more fully constrain the stratigraphic relationships between glacigenic deposits and cap dolostone units. Stratigraphically and diagenetically well constrained negative $\delta^{13}C$ values in rocks deposited before or during the glacial event would greatly change these conclusions. Isotopic values within the glacial period are viewed as the critical information needed to understand the relationships between deglaciation, transgression, variation in the $\delta^{13}C$ record, and widespread carbonate deposition that these enigmatic cap carbonate units record.

ACKNOWLEDGMENTS

The author wishes to thank Malcolm Wallace for significant contribution to the field work, making the work in the Kimberley Region possible, early discussions on the deep-water interpretation, and critical review of the manuscript, Nicholas Christie-Blick for his critical eye in both field work and review of the manuscript, and Louis Derry for his insightful discussions. The author also wishes to thank Victor Gostin for his supervision during the author's Ph.D. study at the University of Adelaide, from which much of the data was derived. Funding was supplied by an Australian Commonwealth Post-Graduate Research Award, and Magellan Petroleum generously supported field work in the Amadeus and Ngalia Basins. The manuscript was much improved by critical reviews from reviewers Anthony Prave, Mark Pagani, and John Southard, as well as informal reviews by Jay Kaufman, George Williams, Robert Dott, Jr., and Ian Fairchild. Lastly the author wishes to thank Barbara and Jim Rowe for their continuous support and logistic assistance.

REFERENCES

Aitken, J.D., 1991a, Two late Proterozoic glaciations, Mackenzie Mountains, northwestern Canada: Geology, v. 19, p. 445–448.

Aitken, J. D., 1991b, The Ice Brook Formation and the Post-Raptian Late Proterozoic Glaciation, Mackenzie Mountains, Northwest Territories: Geologic Survey of Canada Bulletin 404, 65 p.

Anderson, T.F., and Arthur, M.A., 1983, Stable isotopes of oxygen and carbon and their application to sedimentology and paleoenvironmental problems: Society of Economic Paleontologists and Mineralogists Short Course 10, p. 1–151.

Asmeron, Y., Jacobsen, S.B., Knoll, A.H., Butterfield, N.J., and Swett, K., 1991, Strontium isotopic variations of Neoproterozoic seawater: implications for crustal evolution: Geochimica et Cosmochimica Acta, v. 55, p. 2883–2894.

Banner, J.L., and Hansen, G.N., 1990, Calculation of simultaneous isotopic and trace element variations during water-rock interaction with application to carbonate diagenesis: Geochimica et Cosmochimica Acta, v. 54, p. 445–448.

Banner, J.L., Hansen, G.N., and Meyers, W.J., 1988, Water rock interaction history of regionally extensive dolomites of the Burlington–Keokuk formation (Mississippian): isotopic evidence, *in* Shukla, V., and Baker, P.A., eds., Sedimentology and Geochemistry of Dolostones: SEPM Special Publication 43, p. 97–113.

Berger, W.H., 1982, Increases of carbon dioxide during deglaciation: the coral reef hypothesis: Naturwissenschaften, v. 69, p. 87–88.

Broeker, W.S., 1982, Ocean chemistry during glacial times: Geochimica et Cosmochimica Acta, v. 46, p. 1682–1705.

Christie-Blick, N., Dyson, I.A., and von der Borch, C.C., 1995, Sequence stratigraphy and the interpretation of Neoproterozoic earth history: Precambrian Research, v. 73, p. 3–26.

Christie-Blick, N., von der Borch, C.C., and DiBona, P.A., 1990, Working hypothesis for the origin of the Wonoka canyons (Neoproterozoic), South Australia: American Journal of Science, v. 290-A, p. 295–332.

Christie-Blick, N., Mount, J.F., Levy, M., Signor, P.W., and Link, P.K., 1989, Late Proterozoic and Cambrian tectonics, sedimentation, and record of metazoan radiation in the Western United States: International Geological Congress Field Guide T331: Washington D.C., American Geophysical Union, 113 p.

Cloud, P.E., Wright, L.A., Williams, E.G., Diehl, P. and Walter, M.R., 1974, Giant stromatolites and associated vertical tubes from the upper Proterozoic Noonday Dolomite, Death Valley Region, Eastern California: Geological Society of America Bulletin, v. 85, p. 1869–1882.

Coats, R.P., 1973, Copley, South Australia: Geological Survey of South Australia, Geological Map, Sheet SH 54-9, 1:250,000 scale.

Cowie, J.W., and Brasier, M.D., eds., 1989, The Precambrian–Cambrian Boundary: Oxford Monographs on Geology and Geophysics, Clarendon Press, 213 p.

Deharis, F., Chessell, R., and Jedwab, J., 1980, Discrete suspended particles of barite and the barium cycle in the open ocean: Earth and Planetary Science Letters, v. 49, p. 529–550.

Derry, L.A., Keto, L.S., Jacobsen, S.B., Knoll, A.H., and Swett, K., 1989, Sr isotopic variation in upper Proterozoic carbonates from Svalbard and East Greenland: Geochimica et Cosmochimica Acta, v. 53, p. 2331–2339.

Derry, L.A., Kaufman, A.J., and Jacobsen, S.B., 1992, Sedimentary cycling and environmental change in the Late Proterozoic: Evidence from stable and radiogenic isotopes: Geochimica et Cosmochimica Acta, v. 56, p. 1317–1329.

Deynoux, M., and Trompette, R., 1976, Late Precambrian mixtites: glacial and/or non-glacial? Dealing especially with the mixtites of West Africa: American Journal of Science, v. 276, p. 1302–1315.

Dow, D.B., and Gemuts, I., 1969, Geology of the Kimberley Region; East Kimberley: Australia, Bureau of Mineral Resources, Bulletin of Geology and Geophysics, v. 106, 69 p.

Dromart, G., 1992, Jurassic deep water microbial biostromes as flooding markers in carbonate sequence stratigraphy: Palaeogeography, Palaeoclimatology, Palaeoecology, v. 9, p. 219–228.

Dymond, J., Suess, E., and Lyle, M., 1992, Barium in deep sea sediment: a geochemical proxy for paleoproductivity: Paleoceanography, v. 7, p. 163–181.

Dyson, I.A., and von der Borch, C.C., 1994, Sequence stratigraphy of an incised-valley fill: the Neoproterozoic Sea Cliff Sandstone, Adelaide Geosyncline, South Australia, *in* Dalrymple, R.W., Boyd, R., and Zaitlin, B.A., eds., Incised-Valley Systems: Origin and Sedimentary Sequences: SEPM Special Publication 51, p. 209–222.

Eisbacher, G.H., 1985, Late Proterozoic rifting, glacial sedimentation, and sedimentary cycles in the light of Windermere deposition, Western Canada: Palaeogeography, Palaeoclimatology, Palaeoecology, v. 51, p. 231–254.

Fairbanks, R.G., 1989, A 17,000-year glacio-eustatic sea level record: influence of glacial melting rates on the Younger Dryas event and deep-ocean circulation: Nature, v. 342, p. 637–642.

Fairchild, I.J., 1993, Balmy shores and icy wastes: the paradox of carbonates associated with glacial deposits in Neoproterozoic times: Sedimentology Review, v. 1, p. 1–16.

Fairchild, I.J., and Spiro, B., 1990, Carbonate minerals in glacial sediments: geochemical clues to paleoenvironment, *in* Dowdeswell, J.A., and Scourse, J.D., eds., Glacimarine Environments: Process and Sediments: Geological Society of London Special Publication 53, p. 201–216.

Fairchild, I.J., Hambrey, M.J., Spiro, B., and Jefferson, T.H., 1989, Late Proterozoic glacial carbonates in northeastern Spitsbergen: new insights into the carbonate-tillite association: Geological Magazine., v. 126, p. 469–490.

Fairchild, I.J., and Hambrey, M.J., 1984, The Vendian of NE Spitsbergen: petrogenesis of a dolomite tillite association: Precambrian Research, v. 26, p. 111–167.

Field, B.D., 1991, Paralic and periglacial facies and contemporaneous deformation of the Late Proterozoic Olympic Formation, Pioneer Sandstone and Gaylad Sandstone, Amadeus Basin, central Australia, *in* Korsch, R.J., and Kennard, J.M., eds., Geological and Geophysical Studies in the Amadeus Basin, Central Australia: Australia, Bureau of Mineral Resources, Bulletin 236, p. 127–136.

Friedman, G.H., and Sanders, J.E., 1974, Positive relief bedforms on the modern tidal flat that resemble molds of flutes and grooves; implications for geopetal criteria and for the origin and classification of bedforms: Journal of Sedimentary Petrology, v. 44, p. 181–189.

Grotzinger, J.P., Bowring, S.A., Saylor, B.Z., and Kaufman, A.J., 1995, Biostratigraphic and geochronologic constraints on early animal evolution: Science, v. 270, p. 549–704.

Grotzinger, J.P., and Kasting, J.F., 1993, New constraints on Precambrian ocean composition: Journal of Geology, v. 101, p. 235–243.

HEGENBERGER, W., 1987, Gas escape structures in Precambrian peritidal carbonate rocks: Geological Survey of South-West Africa/Namibia, Communications, v. 3, p. 49–55.

HEGENBERGER, W., 1993, Stratigraphy and sedimentology of the Late Precambrian Witvlei and Nama Groups, East of Windhoek: Geological Survey of Namibia Memoir 17, p. 82.

HOFMANN, H.J., NARBONNE, G.M., AND AITKEN, J.D., 1990, Ediacaran remains from intertillite beds in northwestern Canada: Geology, v. 18, p. 1199–1202.

KAUFMAN, A.J., AND KNOLL, A.H., 1995, Neoproterozoic variations in the C-isotopic composition of sea water: stratigraphic and biogeochemical implications: Precambrian Research, in press.

KAUFMAN, A.J., JACOBSEN, S.B., AND KNOLL, A.H., 1993, The Vendian record of Sr and C isotopic variations in seawater: implications for tectonics and paleoclimate: Earth and Planetary Science Letters, v. 120, p. 409–430.

KAUFMAN, A.J., HAYES, J.M., KNOLL, A.H., AND GERMS, G.B., 1991, Isotopic compositions of carbonates and organic carbon from upper Proterozoic successions in Namibia: stratigraphic variations and the effects of diagenesis and metamorphism: Precambrian Research, v. 49, p. 301–327.

KEMPE, S., AND DEGENS, E.T., 1985, An early soda ocean?: Chemical Geology, v. 53, p. 95–108.

KENDALL, C.G., AND WARREN, J.K., 1987, A review of the origin and setting of tepees and their associated fabrics: Sedimentology, v. 34, p. 1007–1027.

KENNEDY, M.J., 1993, The influence of diapirism and deglaciation on the development of the Neoproterozoic stratigraphy of the Amadeus Basin, central Australia [unpublished Ph.D. thesis]: University of Adelaide, 192 p.

KNOLL, A.H., HAYES, J.M., KAUFMAN, A.J., SWETT, K., AND LAMBERT, I.B., 1986, Secular variation in carbon isotope ratios from the upper Proterozoic succession of Svalbard and east Greenland: Nature, v. 321, p. 832–839.

KNOLL A.H., AND SWETT, K., 1990, Carbonate deposition during the late Proterozoic era: An example from Spitsbergen: American Journal of Science, v. 290-A, p. 104–132.

KNOLL, A.H., AND WALTER, M.R., 1992, Latest Proterozoic stratigraphy and earth history: Nature, v. 356, p. 673–678.

KUMP, L.R., 1991, Interpreting carbon-isotope excursions: Strangelove oceans: Geology, v. 19, p. 299–302.

LINK, P.K., 1983, Glacial and tectonically influenced sedimentation in the upper Proterozoic Pocatello Formation, southeastern Idaho, *in* Miller, D.M., Todd, V.R., and Howard, K.S., eds., Tectonic and Stratigraphic Studies in the Eastern Great Basin: Geological Society of America Memoir 157, p. 165–181.

MAGARITZ, M., 1985, The carbon isotope record of dolostones as a stratigraphic tool: a case study from the upper Cretaceous shelf sequence, Israel: Sedimentary Geology, v. 216, p. 249–256.

NARBONNE, G.M., KAUFMAN, A.J., AND KNOLL, A.H., 1994, Integrated chemostratigraphy and biostratigraphy of the upper Windermere Supergroup (Neoproterozoic), northwestern Canada: Implications for Neoproterozoic correlations and the early evolution of animals: Geological Society of America Bulletin, v. 106, p. 1281–1292.

OPDYKE, B.N., AND WALKER, J.C.G., 1992, Return of the coral reef hypothesis: basin to shelf partitioning of $CaCO_3$ and its effect on atmospheric CO_2: Geology, v. 20, p. 733–736.

PAYTAN, A., AND KASTNER, M., 1994, Central equatorial Pacific Holocene sedimentation rates from radium-226 activities in marine barite, (abstract): Eighth International Conference on Geochronology, Cosmochronolgy and Isotope Geology, Abstracts, United States Geological Survey Circular 1107, p. 245.

PLAYFORD, P.E., COCKBAIN, A.E., DRUCE, E.C., AND WRAY, J.L., 1976, Devonian stromatolites from the Canning Basin, Western Australia, *in* Walter, M.R., ed., Stromatolites: Amsterdam, Elsevier, Developments in Sedimentology no. 20, p. 543–564.

PLUMMER, P.S., 1978, Note on the paleoenvironmental significance of the Nuccaleena Formation (upper Precambrian), central Flinders Ranges, South Australia: Geological Society of Australia Journal, v. 25, p. 395–402.

PREISS, W.V., 1987, The Adelaide Geosyncline—Late Proterozoic stratigraphy, sedimentation, palaeontology and tectonics: Geological Society of South Australia Bulletin 53, 438 p.

PREISS, W.V., AND FORBES, B.G., 1981, Stratigraphy, correlation and sedimentary history of Adelaidean (Late Proterozoic) basins in Australia: Precambrian Research, v. 15, p. 255–304.

PREISS, W.V., WALTER, M.R., COATS, R.P., AND WELLS, A.T., 1978, Lithological correlations of Adelaidean glaciogenic rocks in parts of the Amadeus, Ngalia, and Georgina Basins: Australia, Bureau of Mineral Resources, Journal of Australian Geology and Geophysics, v. 3, p. 43–53.

SCHMIDT, P.E., AND WILLIAMS, G.E., 1995, The Neoproterozoic climatic paradox; equatorial paleolatitude for Marinoan Glaciation near sea level in South Australia: Earth and Planetary Science Letters, v. 134, p. 107–204.

SIEDLECKA, A., AND ROBERTS, D., 1992, The bedrock geology of Varanger Peninsula, Finnmark, north Norway: an excursion guide: Norges Geologiske Undersøkelse, Special Publication 5, 45 p.

SMITH, L.H., KAUFMAN, A.J., KNOLL, A.H., AND LINK, P.K., 1994, Chemostratigraphy of predominantly siliciclastic Neoproterozoic successions: a case study of the Pocatello Formation and lower Brigham Group, Idaho, USA: Geological Magazine, v. 3, p. 301–314.

TUCKER, M.E., 1986, Formerly aragonitic limestones associated with tillites in the Late Proterozoic Kingston Peak Formation of Death Valley, California: Journal of Sedimentary Petrology, v. 56, p. 818–830.

TUCKER, M.E., 1983, Diagenesis, geochemistry, and origin of Precambrian dolomite: the Beck Spring Dolomite of eastern California: Journal of Sedimentary Petrology, v. 53, p. 1097–1119.

VEIZER, J., 1983, Chemical diagenesis of carbonates: theory and application of trace element technique, *in* Anderson, T.F., and Arthur, M.A., eds., Stable Isotopes in Sedimentary Geology: Society of Economic Paleontologists and Mineralogists Short Course 10, p. 3.1–3.100.

VAN WAGONER, J.C., MITCHUM, R.M., CAMPION, K.M., AND RAHMANIAN, V.D., 1990, Siliciclastic Sequence Stratigraphy in Well Logs, Cores, and Outcrops: American Association of Petroleum Geologists, Methods in Exploration no. 7, 55 p.

VON DER BORCH, C.C., CHRISTIE-BLICK, N., AND GRADY, A.E., 1989, Depositional sequence analysis applied to Late Proterozoic Wilpena Group, Adelaide Geosyncline, South Australia: Australian Journal of Earth Science, v. 35, p. 59–71.

WALLACE, M.W., KEAYS, R.R., AND GOSTIN, V.A., 1991, Stromatolitic iron oxides; evidence that sea-level changes can cause sedimentary Iridium anomalies: Geology, v. 19, p. 551–554.

WALTER, M.R., AND BAULD, J., 1983, The association of sulfate evaporites, stromatolitic carbonates and glacial sediments: examples from the Proterozoic of Australia and the Cainozoic of Antarctica: Precambrian Research, v. 21, p. 129–148.

WILLIAMS, G.E., 1979, Sedimentology, stable isotope geochemistry and paleoenvironment of dolostones capping late Precambrian glacial sequences in Australia: Geological Society of Australia Journal, v. 26, p. 377–386.

ZEMPOLICH, W.G., WILKINSON, B.H., AND LOHMANN, K.C, 1988, Diagenesis of Late Proterozoic carbonates: the Beck Spring Dolomite of eastern California: Journal of Sedimentary Petrology, v. 58, p. 656–672.

Received 9 June 1995; accepted 29 December 1995.